Convective Instability in a Fluid Mixture Heated from Above

A. La Porta and C. M. Surko
Department of Physics, University of California, San Diego, La Jolla, California 92093
(Received 28 October 1997)

Convection patterns in ethanol-water mixtures with negative ψ are studied when the fluid is heated from above. Although the linear analysis predicts that the instability occurs at zero wave number, a large wave number pattern is observed. The onset is supercritical with a threshold that is experimentally indistinguishable from zero. The convection amplitude exhibits damped oscillations for sudden change in the forcing parameter. At the constant Rayleigh number the patterns first coarsen, then exhibit growth of narrow plumes. The instability appears to be related to salt fingering. [S0031-9007(98)05952-3]

PACS numbers: 47.20.Bp, 47.20.Ky, 47.54.+r

When a fluid mixture is driven far from equilibrium by the flow of heat or material into one or more surfaces of the fluid volume, the system may become unstable to a convective flow which enhances the material and heat transport. There are many important examples of this type of flow in nature and technology. For instance, thermohaline convection in the oceans can be driven by temperature gradients or by salinity gradients [1], and double diffusive convection can be important in crystal growth. Finally, convection in fluid mixtures continues to be an important model system for the study of pattern formation in systems driven far from equilibrium [2].

In this Letter, we describe experiments on convection in a fluid mixture with negative separation ratio in which the fluid is heated from *above*, a regime of parameters which has not been studied extensively. We find that a short wavelength convection pattern appears, despite the fact that the linear instability occurs at zero wave number. The onset of the pattern appears to be supercritical bifurcation to a steady flow, although damped oscillations in the pattern amplitude are observed when the forcing parameter is changed rapidly. The patterns continue to undergo stochastic motion even after they have reached a statistically stationary state.

The experiments were performed in the Rayleigh-Bénard configuration, in which a thin layer of fluid mixture is confined between horizontal plates which are held at a fixed temperature difference. The thermal driving of the system is characterized by the Rayleigh number,

$$\mathrm{Ra} = \frac{g\alpha h^3 \Delta T}{\kappa \nu}, \tag{1}$$

where ν is the viscosity, κ is the thermal diffusivity, g is the acceleration of gravity, α is the thermal expansion coefficient, and h is the cell height. (Below, we will use the reduced Rayleigh number, $r \equiv \mathrm{Ra}/1708$, which is normalized to the onset of convection in a pure fluid.) In principle, it would be simplest to impose similar boundary conditions on temperature and concentration by fixing the concentration difference between the top and bottom plates. In laboratory experiments, however, the system boundaries are typically impermeable to both components of the fluid mixture, so that only the average concentration of solute in the fluid is directly controllable. The Soret effect introduces a coupling between concentration transport and the local temperature gradient in the mixture, and this causes a concentration gradient to develop when a temperature gradient is imposed on the fluid layer.

The strength of the Soret forcing in mixtures is parametrized by the separation ratio,

$$\psi = -c(1 - c) S_t \frac{\beta}{\alpha}, \tag{2}$$

where S_t is the Soret coefficient, c is the concentration, and β is the concentration expansion coefficient [3]. The separation ratio is the ratio of the concentration-induced density gradient to the temperature-induced density gradient in the quiescent state. The remaining quantities required to specify the system are the Prandtl number, $\mathrm{Pr} = \nu/\kappa$, and the Lewis number, $\mathcal{L} = D_c/\kappa$, where D_c is the mass diffusion coefficient.

Ethanol-water mixtures are very convenient for studying Soret-driven flows, because the separation ratio can be varied over a wide range by changing the average ethanol concentration. For typical experimental conditions $5 < \mathrm{Pr} < 11$ and $\mathcal{L} \approx 10^{-2}$. If $c > 0.29$, $\psi > 0$, and the temperature driven density gradient and the concentration driven density gradient have the same sign [3]. In this case, convection occurs only for $r > 0$ (heating from below). Above onset, the flow takes the form of a square pattern with wave number $k \approx \pi/h$ [4,5].

The situation is qualitatively different when $c < 0.29$, for which $-0.7 < \psi < 0$ [3]. In this case, the density gradients arising from the temperature and concentration fields oppose each other. For the well-studied case of $r > 0$ (heating from below), the density gradient arising from the temperature field is destabilizing, and the density gradient arising from the concentration field is weakly stabilizing. For $\mathcal{L} \ll 1$, the onset is a Hopf bifurcation, and the convection pattern takes the form of nonlinear traveling waves [6–9].

The experiments described here were performed at $r < 0$, so that the fluid layer was heated from above. The mixture consisted of 8% ethanol (by weight) in water at

an average temperature of 25 °C, for which $\psi = -0.24$ and Pr = 9. Heating from above, the imposed temperature gradient contributes a stabilizing density gradient. In the quiescent state, the Soret effect generates a destabilizing concentration gradient only about $\frac{1}{4}$ as strong, so the net density gradient in the quiescent state is stabilizing [10,11].

The experiments were performed in a convection cell having a diameter of 21 cm and a height of 0.4 cm, which has been described previously [12], but which has been modified to operate at either positive or negative Rayleigh numbers. The top plate temperature is fixed by a regulated flow bath, and the bottom plate may be heated or cooled using a flow of chilled air from a heat exchange in combination with a film heater attached to the bottom plate. Temperature regulation of the bottom plate is achieved using linear feedback to the film-heater current under constant air cooling. The visualization of the pattern is accomplished using a white-light shadowgraph. The characteristic time scales associated with the system are the vertical thermal diffusion time, $\tau_T = h^2/\kappa = 124$ s, the vertical mass diffusion time, $\tau_c = h^2/D_c = 1.6 \times 10^4$ s, and the vertical viscous damping time, $\tau_v = h^2/\nu = 13.5$ s.

To create the pattern shown in Fig. 1, the Rayleigh number was changed smoothly from zero to a value of -2 over 300 s. Approximately 1600 s after temperature slewing was initiated, the convection pattern shown in Fig. 1 rapidly appeared, then faded. This was followed by two more pulses of convection before the pattern settled down to a constant amplitude after about 5000 s, i.e., a time interval comparable to τ_c. The pattern observed when the amplitude first stabilized was very similar to the initial pattern shown in Fig. 1.

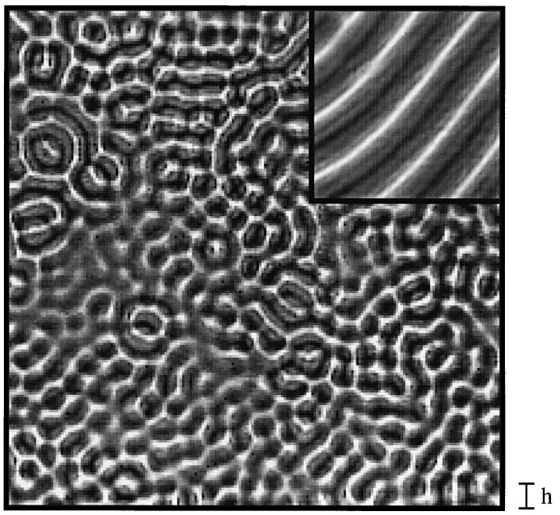

FIG. 1. Convection pattern recorded 1600 s after the reduced Rayleigh number was suddenly set to a value of -2. For comparison, the inset shows a small area of a pattern recorded at the positive Rayleigh number. The distance h indicates the cell height for both patterns.

The time dependence of the pattern amplitude is shown in Fig. 2. The amplitude was measured by subtracting the shadowgraph image of the pattern from a reference image, and calculating the rms value of the difference field. The shadowgraph was operated in a regime in which the intensity modulations in the image depend linearly on the refractive index variations in the fluid. The solid curve in Fig. 2 is seen to rise from zero to a sharp peak at $t = 1600$ s, the time at which Fig. 1 was recorded. The subsequent time trace of the amplitude resembles the response of a damped oscillator. Figure 2 also shows data for sudden onsets at $r = -1.0$ and $r = -0.5$. For weaker forcing, the pattern dynamics are qualitatively similar, although the temporal frequency and the damping rate of the oscillations vary with r.

The pattern observed in Fig. 1 is dramatically different from the normal case of heating from below, as can be seen by comparing the negative-r pattern in Fig. 1 with a positive-r pattern shown in the inset. The main difference appears to be that the negative-r patterns have a much smaller characteristic distance scale. The peak wave number of the negative-r pattern, shown in Fig. 3, also depends on r. Although the linear instability is predicted to be to a zero wave number mode [13], recent calculations indicate that a wide spectrum of wave numbers becomes unstable for strong forcing [14]. The measured dependence of the wave number on r closely corresponds to the most unstable Fourier mode of the linearized system, as calculated by Jung and Lücke [14].

It is possible to explain the large wave number of the negative-r patterns by a simple physical argument. If a convective flow is to occur, up-flows or down-flows must sustain themselves, rather than decay with time. When the system is heated from above and cooled from below, an up-flow draws cold, ethanol-rich fluid up from the bottom of the convection cell. Because of the strong thermal expansion, the fluid drawn up is initially denser than the surrounding fluid and would normally be driven down by the buoyancy force. However, the thermal diffusivity is much larger than the concentration diffusivity in the

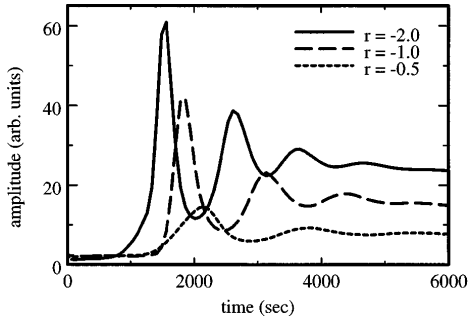

FIG. 2. The rms pattern amplitude as a function of time after a sudden application of the negative Rayleigh number at $t = 0$. The three curves correspond to r values of -2.0 (solid line), -1.0 (long-dashed), and -0.5 (short-dashed).

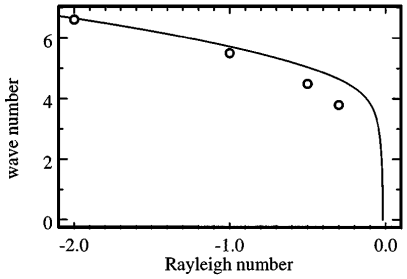

FIG. 3. Circles indicate the peak wave number as a function of the Rayleigh number, measured for sudden application of forcing. The line indicates the most unstable wave number in the linear system, calculated by Jung and Lücke.

mixture. If the flow is sufficiently narrow (i.e., for a large wave number) thermal diffusion would dissipate the horizontal temperature gradients in the up-flow. The concentration gradient is dissipated to a much lesser degree, and so the upwelling fluid would be lighter than the surrounding fluid by virtue of its higher ethanol concentration. Buoyancy associated with this updraft of ethanol-rich fluid can sustain the convective flow. Similar arguments apply to down-flows of hot, ethanol-poor water from the top of the cell. The mechanism involved appears to be closely related to the phenomenon of salt fingering in oceanographic flows [1]. This argument applies in the bulk of the fluid. Close to onset the boundary conditions exert a stronger influence. The result is the selection of a longer wavelength mode [14], as illustrated by the theoretical curve in Fig. 3.

Although the rms amplitude of the pattern remains fairly stable after the initial transient, the pattern continues to evolve with time. In Fig. 4 the convection pattern is shown after the system has been held at $r = -2$ for 4.3×10^4 s. The shadowgraph image still exhibits narrow bright and dark regions, indicating that transport takes place in narrow up-flows and down-flows, but now the separation of the up-flows and down-flows is much larger than their width. While the initial pattern reflects the exponential growth of Fourier modes arising from the linear instability, the late patterns appear to result from nonlinear interactions of the modes. Patterns such as those shown in Fig. 4 do not exhibit any clear symmetry; the lattices formed by the dark and light lines appear to form mostly three-, four-, and five-sided polygons in irregular configurations. The patterns observed here are very similar to those obtained in numerical simulations for $\psi > 0$ and $r > 0$ in the Soret regime, in which the concentration driven buoyancy dominates temperature driven buoyancy [14]. These patterns also bear a striking resemblance to those which result from the instability of bimodal convection in high Prandtl number liquids [15].

The length scale continues to grow until it reaches an upper limit, and a new instability is observed. Weak up-flows and down-flows begin to invade the large quiescent regions. The resulting patterns, such as that shown in Fig. 5, bear a resemblance to dendritic growth. These patterns are not stationary. The smaller up-flows and down-flows move across the pattern in a stochastic manner with a velocity of the order of $0.01h\,\mathrm{s}^{-1}$.

The amplitude of the patterns is shown as a function of r in Fig. 6. The points marked with circles indicate the steady state convection amplitude measured 3×10^4 s after convection was suddenly initiated as in Fig. 2. The square symbols represent the convection amplitude resulting from a gradual application of the forcing over a period of at least 5×10^4 s. In this case transients such as those seen in Fig. 2 are avoided. The triangles indicate the pattern intensity as the Rayleigh number was continuously ramped from $r = -2$ to $r = 0$ over a period of 1×10^5 s.

These data are consistent with a supercritical onset and a linear dependence of the long-time pattern amplitude

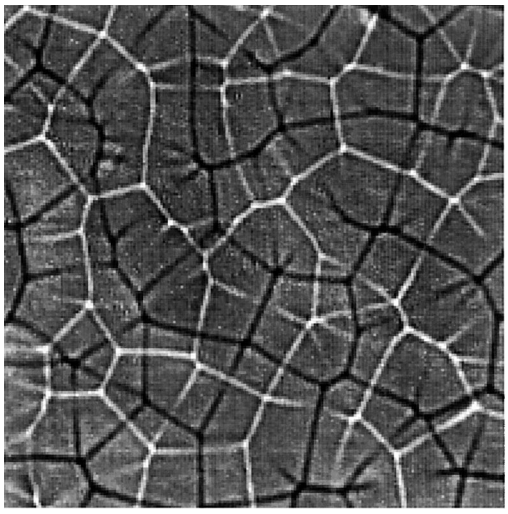

FIG. 4. The development of the convection pattern in Fig. 1 after maintaining $r = -2$ for 4.3×10^4 s.

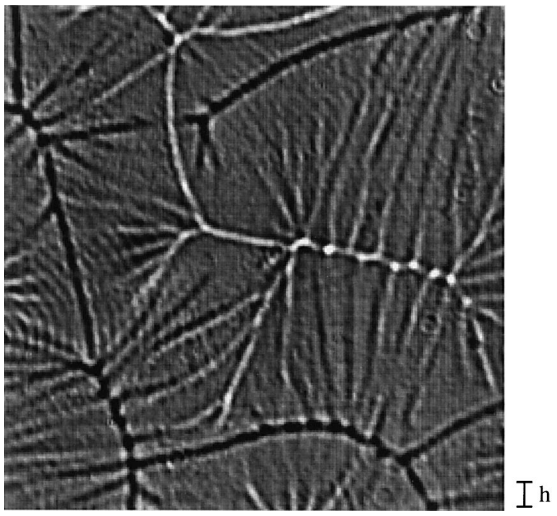

FIG. 5. The convection pattern after continuous evolution at $r = -2.0$ for 6.1×10^5 s (1 week).

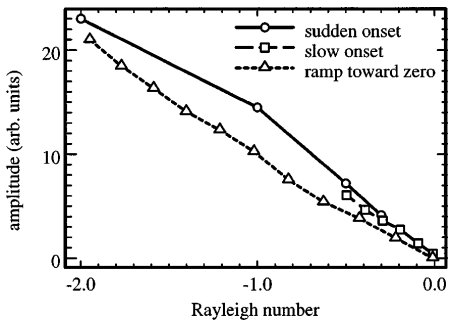

FIG. 6. The amplitude of the pattern as a function of r as described in the text.

on the Rayleigh number. Visualization of the patterns near the onset is difficult because the amplitude is small and broadly distributed in a wave number. The smallest forcing at which a pattern was observed was $r = -0.10$. In this case, visualizing the pattern required averaging 64 frames.

The results presented above can be compared with the linear stability analysis for this system [13,14,16]. For $\mathcal{L} = 10^{-2}$ and $\psi = -0.24$, the critical Rayleigh number is predicted to be $r_c = -0.017$. This value is below our experimental resolution, but is consistent with the data shown in Fig. 6. The experiments confirm that the instability is to stationary convection, but the amplitude is strongly underdamped (see Fig. 2).

The linear stability analysis predicts that the critical wave number is zero [16], although further investigation has revealed that a broad spectrum of wave numbers becomes unstable slightly above threshold [14]. The initial patterns, such as the one shown in Fig. 1, seem to reflect the dynamics of modes in the linearized system, whereas the late patterns, such as those shown in Figs. 4 and 5, presumably result from nonlinear interaction of the modes. In the latter regime, the patterns seem to exhibit two distinct length scales. There is a short length scale, which can be taken to be the lateral extent of an up-flow or down-flow. Using the data of Figs. 1 or 3, this length scale is found to be approximately $h/2$. There is also a longer length scale, which is the average distance between the up-flows and down-flows in the late-time pattern. Based on the data in Figs. 4 and 5, this longer length scale is approximately $3h$. For conventional Rayleigh-Bènard convection, these two length scales are the same and equal to h.

In conclusion, we have observed an instability which occurs when a mixture having negative separation ratio is heated from above. This instability has a number of intriguing features. The amplitude of convection executes damped oscillations when the forcing parameter is changed. The initial pattern reflects the spectrum of the linear instability, although nonlinear interactions subsequently drive it toward a longer wavelength. For very long times, the patterns exhibit persistent stochastic motion. This system appears to be closely related to salt fingering in thermohaline convection, and may be a useful laboratory system for studying this phenomenon.

We thank Ch. Jung and M. Lücke for sharing their unpublished calculations with us and for useful discussions. We also acknowledge useful discussions with J. A. Whitehead. This work is supported by the U.S. Department of Energy under Grant No. DE-FG03-90ER14148.

[1] R. W. Schmitt, Sci. Am. **272**, 70 (1995).
[2] M. C. Cross and P. C. Hohenberg, Rev. Mod. Phys. **65**, 851 (1993).
[3] P. Kolodner, H. Williams, and C. Moe, J. Chem. Phys. **88**, 6512 (1988).
[4] E. Moses and V. Steinberg, Phys. Rev. E **43**, 707 (1991).
[5] M. A. Dominguez-Lerma, G. Ahlers, and D. S. Cannell, Phys. Rev. E **52**, 6159 (1995).
[6] M. C. Cross and K. Kim, Phys. Rev. A **38**, 529 (1988).
[7] E. Knobloch and D. R. Moore, Phys. Rev. A **37**, 860 (1988).
[8] P. Kolodner and C. M. Surko, Phys. Rev. Lett. **61**, 842 (1988).
[9] A. La Porta and C. M. Surko, Phys. Rev. E **55**, R6327 (1997).
[10] J. K. Platten and J. C. Legros, *Convection In Liquids* (Springer-Verlag, Berlin, 1984).
[11] D. Platten, J. K. Villers, and J. C. Legros, in *Laser Anemometry in Fluid Mechanics*, edited by R. J. Adrian *et al.* (Ladoan, Lisbon, 1988), pp. 245–260.
[12] A. La Porta and C. M. Surko, Phys. Rev. E **53**, 5916 (1996).
[13] W. Barten, M. Lücke, M. Kamps, and R. Schmitz, Phys. Rev. E **51**, 5636 (1995).
[14] Ch. Jung and M. Lücke (private communication); Ch. Jung, Ph.D. thesis, Universität des Saarlandes, 1997.
[15] J. Whitehead, J. A. Parsons, and B. Parsons, Geophys. Astrophys. Fluid Dyn. **9**, 201 (1977).
[16] S. Hollinger and M. Lücke, Phys. Rev. E **52**, 642 (1995).